

Spectroscopic and volumetric characterization of a non-microporous amorphous ice

C. Manca, C. Martin, P. Roubin *

*Physique des Interactions Ioniques et Moléculaires UMR 6633, Université de Provence, Centre Saint Jérôme (service 242),
FR-13397 Marseille Cedex 20, France*

Received 22 May 2002; in final form 22 July 2002

Abstract

The aim of this Letter is to re-investigate the characterization of ice porosity. N₂, CH₄ and Ar adsorption on amorphous ice has been compared to that on crystalline ice at low temperatures, using adsorption isotherm volumetry and infrared spectroscopy simultaneously. Here we show that amorphous ice can present a large specific surface area and nevertheless be non-microporous; this provides new ways for the understanding of interstellar reactivity.

© 2002 Elsevier Science B.V. All rights reserved.

Amorphous ice is one of the major components of interstellar grain mantles and has proved to play a key role in the formation of astrophysical molecular species [1–6]. It can be obtained in laboratory below 140 K and has been the subject of many studies to determine its physical properties and structure [7–14]. They have shown that amorphous ice generally has a large specific surface area (more than 100 m² g^{−1}) as proved for example by the large adsorption capacity found by isotherm measurements [7,9,10,15]. These large specific surface areas have generally been explained by the existence of micropores. As a matter of fact, micropore diameter is lower than 2 nm and microporous samples have thus a large specific surface area; in addition, adsorption energies in

such pores are enhanced by a confinement effect. To our knowledge, Mayer and Pletzer [7] have performed the most suitable experiments, i.e., adsorption isotherm volumetry, to prove the presence of micropores, using N₂ to probe the ice surface. We have performed similar experiments on our samples, comparing N₂, CH₄ and Ar behaviors and in addition, volumetry has been coupled with infrared spectroscopy.

‘ α_s -plot’ [16] is an empirical method allowing a semi-quantitative analysis of microporosity. It consists in plotting the amount of gas adsorbed on the sample as a function of that measured at the same pressure on a material similar, but non-porous and taken as reference. If the sample is also non-porous, adsorptions are similar on both materials and the adsorbed amounts are proportional: the plot is a straight line. Conversely, for a microporous sample, deviation from linearity at the beginning of adsorption is observed: the

* Corresponding author.

E-mail address: proubin@piimal.univ-mrs.fr (P. Roubin).

expected enhanced interaction for molecules confined in micropores lead to an enhanced adsorbed amount. After micropore filling, adsorption occurs on the external surface (i.e., non-microporous surface) and the plot is merely a straight line. The specific surface area of the external surface can be estimated from this linear part, giving an estimation of the relative weight of the microporous and non-microporous surfaces.

Amorphous ice samples were prepared as follows: a gaseous mixture $\text{H}_2\text{O}:\text{Ar}$ (1:30) was sprayed into a cell held at 40 K, then slowly annealed up to 90 K in order to eliminate argon [17]. In such conditions, using temperature below 130 K, our samples are expected to be amorphous. Their characterization was performed simultaneously by Fourier transform infrared spectroscopy and adsorption isotherm volumetry. The spectra were recorded with a NICOLET 7199 FTIR spectrometer and the resolution was 1 cm^{-1} .

The infrared spectrum at 93 K (Fig. 1) compares well with those already published for amorphous ice [18–21], confirming the validity of the method for preparing ice; the amorphous nature is characterized by the shape of the broad band centered at roughly 3250 cm^{-1} due to OH stretching motions coupled by the strong hydrogen bond network, and by the weak band at 3696 cm^{-1} due to

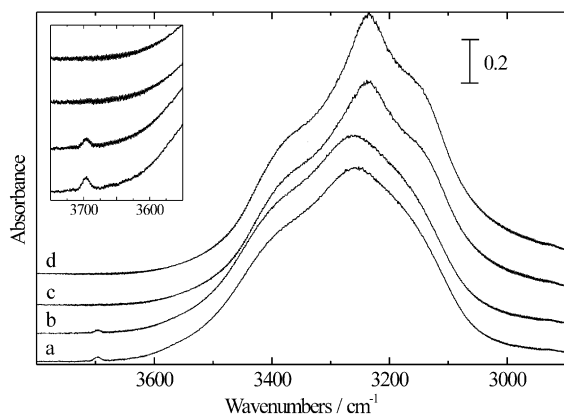


Fig. 1. Infrared spectra of ice in the OH stretching region: (a) $T = 93\text{ K}$, (b) 122 K , (c) 147 K and (d) 165 K . The spectra are offset for clarity and the dangling OH bond region is plotted in the inset in an extended scale.

low-coordinated surface molecules which have a dangling OH bond [22].

N_2 , CH_4 and Ar adsorption isotherms were performed at $T = 56, 73$ and 60 K , respectively, in order to get similar values of T/T_c (T_c being the temperature of the critical point), assuming therefore that the three adsorbed phases presented similar mobility on the surface. At the end of the experiment, the gas was totally desorbed and the sample was then annealed at 90 K to avoid further contamination before the next experiment. We checked that neither infrared spectrum nor adsorption capacity was modified by successive adsorption–desorption cycles. In Fig. 2a, the adsorbed amount is plotted as a function of relative pressure p/p^0 , p^0 being the saturation pressure.

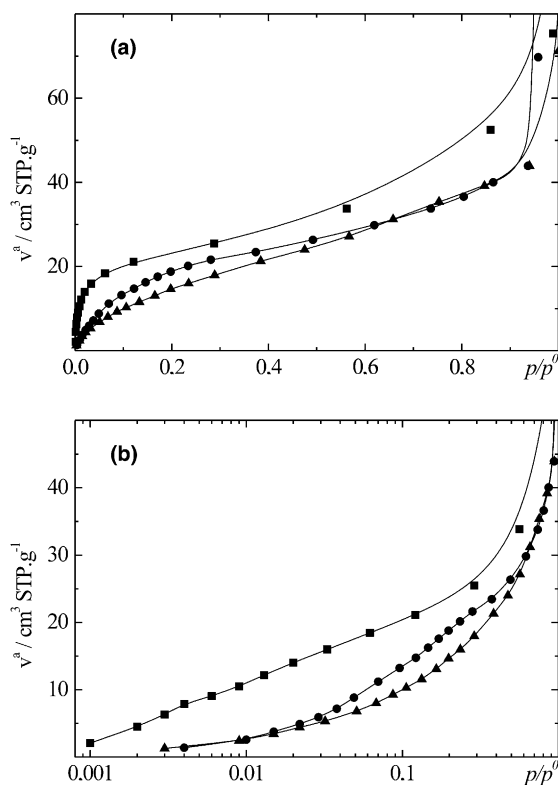


Fig. 2. N_2 (■), CH_4 (●) and Ar (▲) isotherms were performed at $T = 56, 73$ and 60 K , respectively. Adsorbed amount v^a is plotted as a function of relative pressure p/p^0 in (a) a linear scale, (b) an extended logarithmic scale. The solid lines are intended to guide the eye and do not represent a fit of the data.

According to the IUPAC classification [16], N_2 , CH_4 and Ar adsorption isotherms are type II, which is in agreement with previous results [7,10,23]. The ‘step’ at low pressure is caused by the formation of the first layer, whereas the quasi-linear middle section is caused by a multilayer formation, the bulk condensation being at $p/p^0 = 1$. We used the B.E.T. method [24] with N_2 as probe molecule (using the value of cross-sectional area at 77 K: 0.162 nm^2) and we obtained specific surface areas between 100 and $300 \text{ m}^2 \text{ g}^{-1}$, and net heat of adsorption $\approx 2.5 \text{ kJ mol}^{-1}$ (the relative pressure range used for the fit was 0.05 – 0.35). We checked that the results presented here for a sample with a $100 \text{ m}^2 \text{ g}^{-1}$ specific surface area – infrared spectra as well as isotherm shapes – were also reproducible for higher specific surface area (up to $300 \text{ m}^2 \text{ g}^{-1}$). We would like to emphasize that, despite the difference in preparing ice, we have obtained same shape of isotherms and similar values of both specific surface area and net heat of adsorption than those previously published [7,15], revealing similar interactions between N_2 and ice. It should be noted that the low value of net heat of adsorption shows that the interactions are surprisingly weak which is non-consistent with the substantial increase in adsorption energy expected in the case of micropore confinement.

The sample was then annealed up to 165 K : Fig. 1 shows the infrared spectra of ice at $T = 93$, 122 , 147 and 165 K . At 122 K , the band due to dangling OH bonds is lower than at $T = 93 \text{ K}$, indicating that the surface has begun reorganizing and that unstable surface sites are disappearing. At 147 K , the main band is clearly 15 cm^{-1} redshifted and a new shoulder appears at 3150 cm^{-1} , indicating that the bulk has crystallized. No other change is observed when the sample is maintained at 165 K ; this shows that this phase is stable, as previously observed by Jenniskens and Blake [25], and we therefore took this crystalline ice as reference for comparison with amorphous ice. N_2 , CH_4 and Ar isotherms were measured on this sample in the same conditions as those before annealing. They are all type II as in the case of amorphous ice, but the adsorbed amount is much lower: the specific surface area is ≈ 6 times lower than that of amorphous ice. As shown by Stevenson et al. [14],

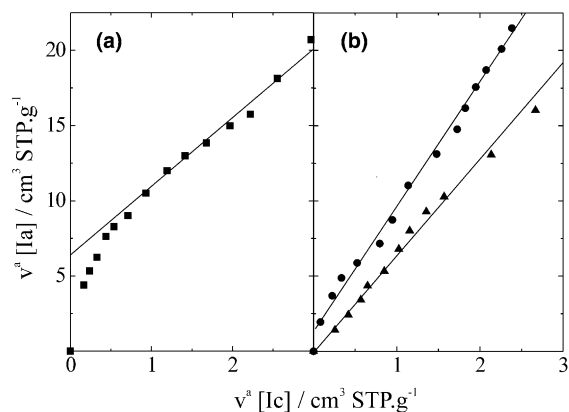


Fig. 3. Correlation between adsorbed amounts measured on amorphous ice ($v^a [\text{Ia}]$) and on crystalline ice ($v^a [\text{Ic}]$): (a) N_2 (■), (b) CH_4 (●) and Ar (▲). The straight lines are guides for the eye.

this ratio can reach 20, depending on the ice preparation conditions.

Fig. 3 shows the adsorbed amount on amorphous ice as a function of that on crystalline ice for the three gases; similar results, not shown here, have been obtained when the reference is ice annealed at 120 K , i.e., before crystallization. In the case of N_2 (Fig. 3a), a deviation from linearity below the monolayer completion is clearly observed, as it was by Mayer and Pletzer [7] who attributed it to the presence of micropores. In contrast, a straight line is obtained in the cases of Ar and CH_4 (Fig. 3b). The non-linearity observed in the case of N_2 is then not due to micropores because it should not be dependent on the probe gas: the three adsorbates have similar cross-sectional areas (0.162 , 0.138 and 0.177 nm^2 for N_2 , Ar and CH_4 , respectively [16]) and if micropores are probed by N_2 , they should be probed by CH_4 and certainly by Ar which is smaller than N_2 . To confirm that this deviation is not due to micropores, we have estimated the external surface area deduced from the linear part of the curve and found that it is equal to the area deduced from B.E.T. method; this shows that the whole surface is external and that the sample is non-microporous. We thus believe that the deviation from linearity observed in Fig. 3a is more likely due to specific interactions of N_2 with amorphous ice

caused by its quadrupole moment. We have already observed a special behavior for both CO and N₂ when comparing the adsorption of these two molecules with that of spherical molecules [26]. The work of Storck et al. [27] concerning other surfaces has led to similar conclusions about the special behavior of N₂, leading to the conclusion that N₂ is not suitable for probing microporosity.

The difference in the behavior observed in the case of N₂ for crystalline and amorphous surfaces is explained by the difference in the nature of these two surfaces. In fact, it has been shown [28] that the free OH coverage on the surface of crystalline ice is much less (approximately one-sixth) than that on amorphous ice. These sites are the less bonded of the surface sites and are thus the first to disappear when heating the sample. In the same way, they are the most reactive and should play a key role in adsorption features, especially for low coverage.

Another indication of non-microporosity is given by the shape of the step observed in Fig. 2a; a microporous sample gives rise to a much sharper step appearing at lower pressure and with an inflection point in the logarithmic plot of the isotherm [27]; this is clearly not observed in Fig. 2b. Net heat of adsorption values have been deduced from previous experiments by fitting the shape of the step using the B.E.T. method [26] and have been found to be much lower ($<3 \text{ kJ mol}^{-1}$) than those expected if there are micropores, which lead to confinement interaction enhancement ($>10 \text{ kJ mol}^{-1}$) [29]. The entire shape of the isotherms must also be taken into account; according to Rouquerol et al. [16], type II isotherms are typically observed in the case of non-porous or macroporous samples. Microporous samples should lead to type I isotherms (i.e., presenting a horizontal plateau), but reciprocally, obtaining a type I isotherm is not sufficient to prove microporosity.

It should be noted that amorphous ice is a disordered material and may be composed of a size distribution of pores and not only of micropores or of larger pores. In the same way, type II isotherms may include a type I component, possibly due to different types of pores. What we show here by correlating the shape of isotherm, the position of the step, the value of net heat of adsorption, the

comparison of different molecules and their specific interactions, is that the microporous nature is certainly non dominant. Moreover, in all our experiments, the whole amount adsorbed was easily desorbed merely by expanding the gas contained in the cell into vacuum, which confirms the absence of micropores.

The presence of larger pores may also explain the large specific surface area measured but, as Mayer and Pletzer [7], we found no evidence for hysteresis loops during desorption, which would have validated this hypothesis. Conversely, Schmitt et al. [9] have measured a hysteresis loop only for high relative pressure ($p/p^0 > 0.4$), probably due to mesopores or macropores. This puts the stress on the crucial role played by the preparation conditions in the final ice structure. For example, a low temperature deposition and the use of a carrier gas [7,9–11,30] are known to favor amorphous character of ice and high adsorption capacity. Mixing H₂O with argon during the vapor deposition probably does not prevent the clustering of water molecules due to the strong attraction of hydrogen bonding. Our samples may then be constituted of grains and inter-grain cavities. Using the simple model of an assembly of spherical grains and assuming 0.91 g cm^{-3} for the ice absolute density [7], the grain diameter is found to be about 65 nm.

To understand the origin of the species observed in the interstellar medium, reactions involving adsorbed species on icy grain mantles have been proposed since exchanges may occur between gas phase and adsorbed molecules. Up to now, the expected microporous structure of ice has been supposed to make the trapping of molecules efficient. The main example is the H₂ recombination mechanism [7] in which micropores play the role of gas storage: during warm up, ice recombination and reduction of surface area may occur, and therefore gas filling micropores may desorb and react in the gas phase, or be trapped in the bulk of ice by pore closure. An opened surface would conversely prevent from trapping in close pore: residence time of adsorbed molecules may be shorter than in the case of porous confinement, but diffusion may be more efficient. Such a surface would favor reactions between adsorbed molecules

by providing a larger free surface for collisional reactivity than in a complex pore network. For instance, C, N, O and S atoms can diffuse on the surface until they find an adsorbed co-reactant and various reactions can occur, needing weaker activation energy than in the case of porous surface. This mechanism may play a role in explaining the high abundances of molecules as NH_3 , H_2CO or CH_3OH in the outer regions of interstellar clouds.

To conclude, we would like to emphasize that the existence of large specific surface areas is not sufficient to conclude on the microporosity of the samples. We have shown here that ice may be amorphous but non-microporous; the hypothesis of a non-microporous ice may be relevant for interpreting interstellar chemical reactivity.

References

- [1] A.G.G.M. Tielens, W. Hagen, J.M. Greenberg, *J. Phys. Chem.* 87 (1983) 4220.
- [2] T.Y. Brooke, A.T. Tokunaga, H.A. Weaver, J. Crovisier, D. Bockelee-Morvan, D. Crisp, *Nature* 383 (1996) 606.
- [3] V. Buch, J.P. Devlin, in: *Molecules in Astrophysics: Probes and Processes*, Kluwer Academic Publishers, Dordrecht, 1997, p. 321.
- [4] R.L. Hudson, M.H. Moore, *Icarus* 126 (1997) 233.
- [5] M.H. Moore, R.L. Hudson, *Icarus* 135 (1998) 518.
- [6] M.P. Bernstein, S.A. Sandford, L.J. Allamandola, J.S. Gillette, S.J. Clemett, R.N. Zare, *Science* 283 (1999) 1135.
- [7] E. Mayer, R. Pletzer, *Nature* 319 (1986) 298.
- [8] D. Laufer, E. Kochavi, A. Bar-Nun, *Phys. Rev. B* 36 (1987) 9219.
- [9] B. Schmitt, J. Ocampo, J. Klinger, *J. de Physique* 48 (1987) C1.
- [10] R. Pletzer, E. Mayer, *J. Chem. Phys.* 90 (1989) 5207.
- [11] W. Langel, A. Becker, H.-W. Fleger, E. Knözinger, *J. Mol. Struct.* 297 (1993) 407.
- [12] A.I. Kolesnikov, J.-C. Li, S. Dong, *Phys. Rev. Lett.* 79 (1997) 1869.
- [13] M.S. Westley, G.A. Baratta, R.A. Baragiola, *J. Chem. Phys.* 108 (1998) 3321.
- [14] K.P. Stevenson, G.A. Kimmel, Z. Dohnalek, R.S. Smith, B.D. Kay, *Science* 283 (1999) 1505.
- [15] B. Schmitt, Ph.D. thesis, Université scientifique technologique et médicale, Grenoble, November, 1986.
- [16] F. Rouquerol, J. Rouquerol, K. Sing, *Adsorption by Powders and Porous Solids*, Academic Press, London, 1999.
- [17] C. Manca, C. Martin, A. Allouche, P. Roubin, *J. Phys. Chem. B* 105 (2001) 12861.
- [18] W.G. Madden, M.S. Berggren, R. McGraw, S.A. Rice, M.G. Sceats, *J. Chem. Phys.* 68 (1978) 3497.
- [19] J.P. Devlin, V. Buch, *J. Phys. Chem.* 99 (1995) 16534.
- [20] A. Allouche, P. Verlaque, J. Pourcin, *J. Phys. Chem. B* 102 (1998) 89.
- [21] J.P. Devlin, J. Sadlej, V. Buch, *J. Phys. Chem. A* 105 (2001) 974.
- [22] V. Buch, J.P. Devlin, *J. Chem. Phys.* 94 (1991) 4091.
- [23] N. Nair, A. Adamson, *J. Phys. Chem.* 74 (1970) 2229.
- [24] S. Brunauer, P. Emmet, E. Teller, *J. Am. Chem. Soc.* 60 (1938) 309.
- [25] P. Jenniskens, D.F. Blake, *Science* 265 (1994) 753.
- [26] C. Martin, C. Manca, P. Roubin, *Surf. Sci.* 502-503C (2002) 275.
- [27] S. Storck, H. Bretinger, W.F. Maier, *Appl. Catal. A* 174 (1998) 137.
- [28] J.E. Schaff, J.T. Roberts, *J. Phys. Chem.* 100 (1996) 14151.
- [29] J. Rouquerol, F. Rouquerol, Y. Grillet, *Pure Appl. Chem.* 61 (1989) 1933.
- [30] E. Mayer, R. Pletzer, *J. Chem. Phys.* 80 (1984) 2939.